Cuts	ν_τ Eff. (%)	ν_e CC	$\bar{\nu}_e$ CC	ν_τ CC $\Delta m^2 = 10^{-3}$ eV^2	ν_τ CC $\Delta m^2 = 3.5 \times 10^{-3}$ eV^2	ν_τ CC $\Delta m^2 = 10^{-2}$ eV^2
Initial	100	437	29	9.3	111	779
Fiducial volume	88	383	25	8.2	97	686
One candidate with momentum > 1 GeV	72	365	25	6.7	80	561
$E_{vis} < 18$ GeV	67	64	5	6.2	75	522
$P_T^e < 0.9$ GeV	54	31	3	5.0	60	421
$P_T^{lep} > 0.3$ GeV	51	29	2	4.7	56	397
$P_T^{miss} > 0.6$ GeV	33	4	0.4	3.1	37	257

Table 5.7: Rejection of the ν_e CC background in the $\tau \to e$ analysis. Figures are normalized to an exposure of 20 kton × year.

a τ decay where the total τ energy must be shared with two additional final state neutrinos. As shown in Figure 5.12, oscillated events tend to accumulate at relatively low values of P_T^e, therefore an upper cut on P_T^e efficiently removes background. We define P_T^{lep} as the transverse momentum of the electron candidate with respect to the jet direction. The lower cut on P_T^{lep} removes events where the candidate electron is not isolated from the hadronic jet. Since this cut is suppressing NC backgrounds, it will be discussed in more detail in the following section.

The final discrimination is achieved with a cut on the transverse missing momentum in the plane perpendicular to the incoming neutrino direction (P_T^{miss}). As Figure 5.13 shows, ν_e CC events are well balanced and very few populate the high P_T^{miss} region, where the bulk of the signal is expected. Requiring $P_T^{miss} > 0.6$ GeV, 65% of the remaining signal events are kept while only 14% of the remnant background survives.

In Table 5.7 we summarize the list of sequential cuts applied to reduce the ν_e and $\bar{\nu}_e$ CC backgrounds and the expected number of signal events for three different Δm^2 values. The most sensitive analysis predicts, for a 20 kton × year exposure, a total background of 4.4 events for a total τ selection efficiency of 33%.

ν *NC* **rejection**

Neutral current events contribute to the background from two sources:

1. electrons from Dalitz decays
2. misidentified charged and neutral pions ($e/\pi^\pm$ and e/π^0 discrimination).

To evaluate the kinematical reduction of the background due to neutral pion misidentification, every photon from π^0 decays, converting within 2 cm (corresponding to 6 readout wires) of the primary interaction vertex is considered as a potential electron candidate. Photons converting beyond 2 cm will be clearly identified by the imaging.

An additional source of background, we denote as $\pi \to e$, arises from early interacting charged pions accompanied by subsequent π^0 production. The probability to misidentify

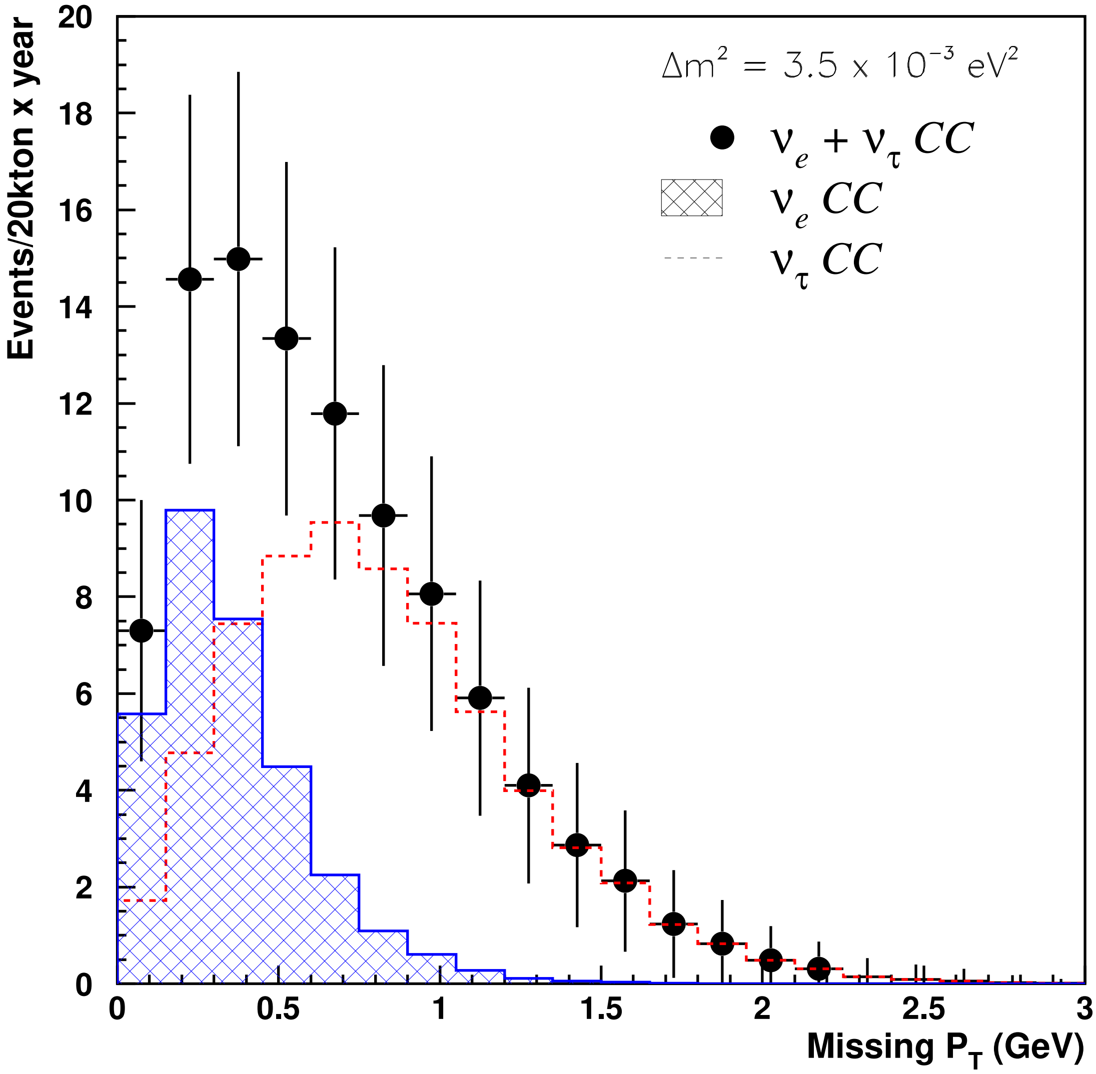

Figure 5.13: Missing total transverse momentum for ν_e CC and ν_τ CC with subsequent $\tau \to e\nu\nu$ decay. Electron channel analysis. Curves are normalized to 20 kton $\times$ year. Successive cuts have been applied.

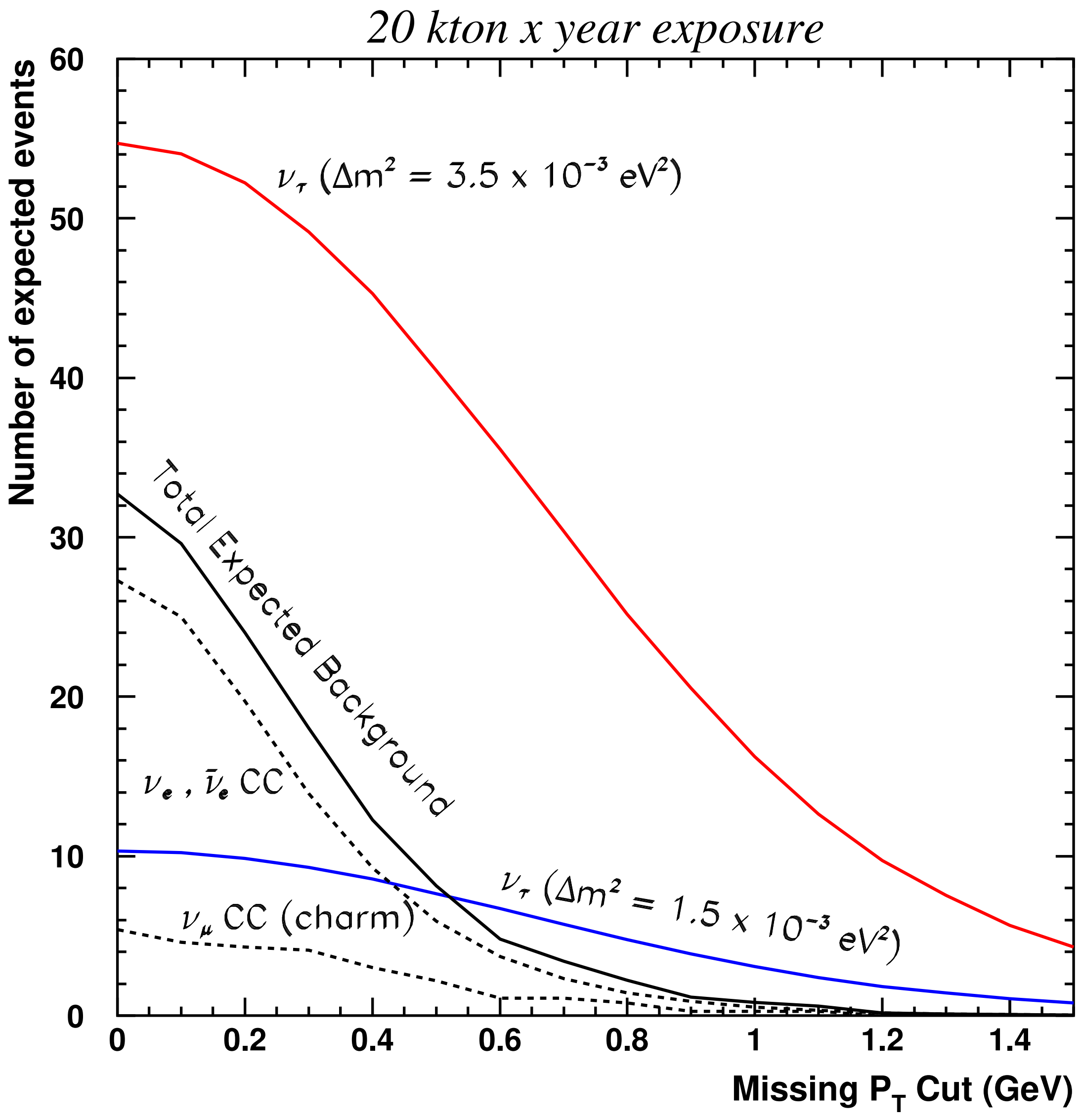

Figure 5.14: Number of ν_e, $\bar{\nu}_e$ background and tau events expected for a 20 kton $\times$ year exposure as a function of the missing transverse momentum.

charged pions as electrons have been obtained through a *full simulation* of interacting pions of different energies inside the liquid target. The criteria used to label an interacting pion as an electron are:

- Pion interaction should take place within a path of $3X_0$ from the primary neutrino interaction vertex. Only 5% of the electrons will not shower before this distance, against a probability of 40% for hadrons not to interact over the same distance.
- There should be at least one π^0 produced in the interaction.
- There should be only one emerging hadronic charged track in the interaction.
- There should be no protons with kinetic energy above 50 MeV emerging from the hadronic secondary interaction. No constraint is imposed on neutrons. In reality, a fraction of exiting neutron can be identified due to their interaction. But we conservatively ignore this possibility.
- The interaction products and the incident pion should be roughly collinear, namely, the angle between the secondary charged pion and the primary one should be less than 100 mrad. Likewise, the angle between π^0 and the primary pion should also be smaller than 100 mrad.

All these requirements provide a $\pi \to e$ misidentification probability factor of 5×10^{-5} for pions of 1.5 GeV of momentum. This value increases with energy, due to the increased collimation of the secondary products, and reaches 7×10^{-3} for pion of 15 GeV momentum. This probability is folded with the momentum spectrum of every charged pion in neutral current events. This yields for an exposure of 20 kton $\times$ year, about seven events where an interacting pion inside the liquid target is misidentified as an electron before kinematical cuts. Kinematics criteria provide additional rejection power, as shown in Table 5.8.

We also study the level of background contamination produced by events where a charged pion, ranging out inside the liquid target, overlaps with late converted photons coming from a π^0 decay. This kind of background is much reduced if we consider that such event topology resembles an electron if and only if the angle between the $\pi^{\pm}$ and the π^0 is less than 10^o. Before any kinematics cuts, we expect 25 events of this kind of background for the exposure considered above.

Table summarizes 5.8 the rejection power of kinematics criteria for the four sources that contribute to ν *NC* background. The requirement on the electron candidate energy $E_e > 1$ GeV suppresses about one third of the Dalitz, pion overlap and π^0 conversions induced backgrounds, since electrons in the jet are soft.

Genuine electrons coming from a τ decay are more isolated than ν_μ NC electron candidates, since these emerge from within the jet. Therefore kinematic variables that strongly depend on the isolation of the candidate are a powerful tool to eliminate NC. A soft cut $P_T^{lep} > 0.3$ GeV reduces Dalitz decays and π^0 background by a factor two while 94% of the τ signal is kept.

From Table 5.8 we observe that kinematics criteria reduce Dalitz induced background by more than one order of magnitude, π^0 misidentification by about a factor eight while the background due to $e/\pi^{\pm}$ confusion is reduced by more than a factor three.

The ultimate discrimination of these backgrounds relies primarily on the imaging capabilities and on dE/dx measurements, as described in chapter 4. We note that dE/dx measurements provide close to three orders of magnitude rejection factor. The combination of dE/dx information together with kinematics criteria is sufficient to reduce ν NC background to a negligible level.

Cuts	ν_μ NC			
Initial	17750			
Fiducial volume	15550			
	Dalitz	γ conversions	$\pi \to e$	$\pi^\pm/\pi^0$ overlap
One candidate	275	4262	6.5	25
$P_e > 1$ GeV	79	1361	6.3	16
$E_{vis} < 18$ GeV	49	835	3.2	11
$P_T^e < 0.9$ GeV	46	794	1.8	9
$P_T^{lep} > 0.3$ GeV	24	429	1.7	8
$P_T^{miss} > 0.6$ GeV	19	350	1.3	7
Imaging and dE/dx	< 1	< 1	< 1	< 1

Table 5.8: ν_μ NC background to the $\tau \to e$ analysis. Results are normalized to an exposure of 20 kton $\times$ year. We illustrate background reduction by means of kinematical criteria only. Imaging and dE/dx measurements reduce the NC background to a negligible level.

ν_μ CC rejection

Charged current events can contribute to the background in a similar way as the neutral current events described above when the leading muon escapes detection.

This situation can happen in the two following cases:

- *Exiting* μ: the energetic leading muon ($< P_\mu > = 8$ GeV) exits through the sides of the liquid target.
- *Stopping* μ: a soft muon ($< P_\mu > = 2$ GeV) decays or ranges out inside liquid argon. The fraction of such muon is 7% of the total.

In case the muon is not identified, the event will appear in first instance as a neutral current event. The source of electrons which can induce backgrounds are then similar to those discussed previously: Dalitz decays, γ conversions and $e/\pi^\pm$ misidentification. They are reduced to a negligible level for reasons already discussed when dealing with NC backgrounds, even though it should be stressed that the kinematical rejection is less efficient for ν_μ CC events than for ν_μ NC events: the misidentification of the muon as a hadron alters the kinematic properties of the "jet".

A more important source of background specific to charged current interactions comes from the decays of charmed mesons. At the CNGS energies $\sigma(\nu_\mu N \to \mu\ c\ X)/\sigma(\nu_\mu N \to \mu X) \approx 4\%$, therefore for a total exposure of 20 kton $\times$ year we expect to collect about 200 events where a charmed meson decays into a positron and a neutrino. These events resemble kinematically the real ν_τ events, since they have a neutrino in the final state and possess a softer energy spectrum and a genuine sizeable missing transverse momentum.

Kinematical criteria reduce contamination due to charm events by a factor $R_{kine} = 7 \times 10^{-2}$ (see Table 5.9). For a 20 kton $\times$ year exposure this translates into 15 expected background events. These criteria alone are insufficient to bring down ν_μ *CC* background to a tolerable level.

The rejection of these charmed events calls for an improved muon "veto". The adopted veto proceeds in two steps:

- To reduce the background labelled as *exiting* μ we adopt the following criteria: tracks that exit the liquid detector and reach the solid part of *ICANOE*, depositing the equivalent of a mip are tagged as muons and the event is rejected. In addition we take advantage of the large dimensions of the detector and its nuclear interaction length (84 cm): thus, every track that exits the active liquid target through the sides without interacting is assumed to be a muon and the event is discarded.

  These criteria reduce ν_μ CC background by a factor $N_{exiting} = 1/4$ for a modest loss of 3% in τ selection efficiency. At this stage 4 background events are expected.

- The veto to reject events with a *stopping* μ proceeds as follows: Tracks followed by an electromagnetic cascade are identified as a muon decay. Moreover, tracks traveling more than 3λ and stopping inside the detector without producing a secondary interaction are identified as muons.

  This veto reduces by factor $N_{stopping} = 1/4$ the remaining ν_μ CC background while the reduction on τ signal efficiency is less than one per cent.

In summary, the expected number of charm induced background events $n^b_{CC\ (charm)}$ for a total exposure of 20 kton $\times$ year is:

$$\boldsymbol{n^b_{CC\ (charm)} = N_{charm} \times R_{kine} \times N_{exiting} \times N_{stopping} = 1}$$

Table 5.10 summarizes the expectations for the $\tau \to e$ analysis once kinematics criteria and muon vetoes have been applied to every potential background source. In conclusion, we obtain for a 20 kton $\times$ year exposure, that the overall electron selection efficiency is 32% for an expected number of about five background events. The expected number of taus at our central Δm^2 value (i.e., 3.5×10^{-3} eV^2) is 35.

5.5.2 Hadronic decay modes

The hadronic decays of the τ can be used to search for $\nu_\mu \to \nu_\tau$ oscillations. The largest background before kinematical cuts comes from ν NC events. Charged current events where the muon is not identified can also be a dangerous background.

The intrinsic missing momentum related to the outgoing neutrino in NC events does not allow to search for these decay modes by selecting the momentum imbalance in the transverse plane like for the $\tau \to e$ channel. For the hadronic channels, the isolation of the candidate is the most discriminating variable against background. Isolation is defined as the transverse momentum of the hadron w.r.t. to the jet direction. A hadron coming

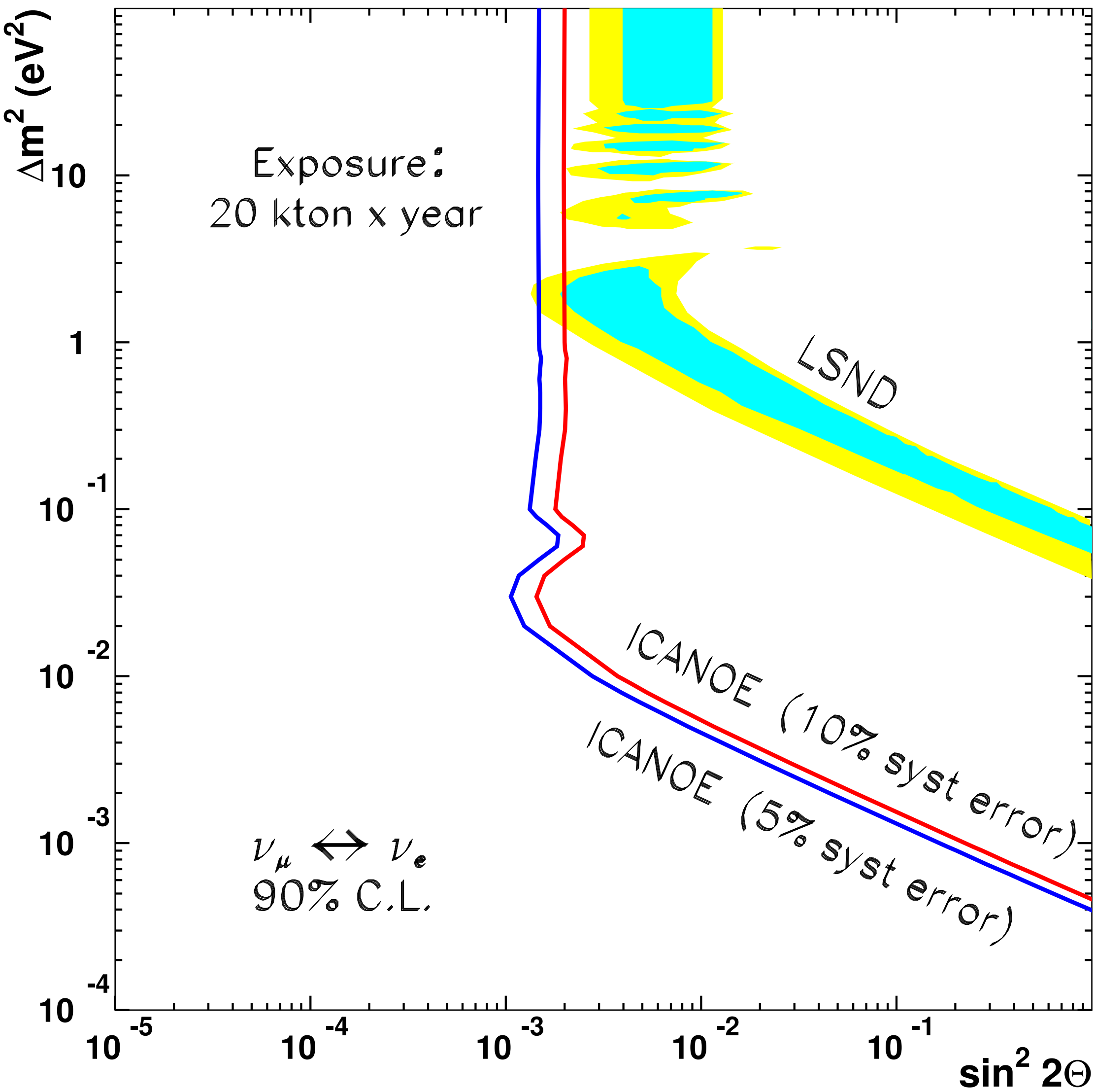

Figure 5.17: *ICANOE* 90% C.L. exclusion region in case no $\nu_\mu \to \nu_e$ are experimentally observed.